DEUTSCHES ELEKTRONEN-SYNCHROTRON
INSTITUT FÜR HOCHENERGIEPHYSIK

DESY 93-089
July 1993

Complete Tree-Level Calculation of the Reaction $e^+e^- \longrightarrow \mu^+\mu^- b\bar{b}$ and the Higgs Boson Signal at LEP200 and NLC Energies

E. Boos

Institute of Nuclear Physics, Moscow State University, Russia

M. Sachwitz, H. J. Schreiber

Deutsches Elektronen-Synchrotron DESY
Institut für Hochenergiephysik IfH, Zeuthen

S. Shichanin

Institute for High Energy Physics, Protvino, Moscow Region, Russia

ISSN 0418-9833

PLATANENALLEE 6 - 15738 ZEUTHEN

To be sure that your preprints are promptly included in the
HIGH ENERGY PHYSICS INDEX,
send them to (if possible by air mail):

DESY **Bibliothek** **Notkestraße 85** **22603 Hamburg** **Germany**	**DESY-IfH** **Bibliothek** **Platanenallee 6** **15738 Zeuthen** **Germany**

DESY 93-089
July 1993

ISSN 0418-9833

Complete Tree-Level Calculation of the Reaction $e^+e^- \longrightarrow \mu^+\mu^- b\bar{b}$ and the Higgs Boson Signal at LEP200 and NLC Energies

E. Boos[1]
Nuclear Physics Institute, Moscow State University, 119899, Moscow, Russia

M. Sachwitz, H. J. Schreiber
DESY Institute für Hochenergiephysik, Zeuthen, FRG

S. Shichanin[1]
Institute for High Energy Physics, 142284, Protvino, Moscow Region, Russia

[1]Supported by a grant from the Ministry of Science, Research and Culture of the State of Brandenburg

Abstract

A complete tree-level calculation of the reaction $e^+e^- \longrightarrow \mu^+\mu^- b\bar{b}$ in the electroweak standard theory for the energy range of LEP200 and the Next Linear Collider is presented. The matrix elements have been calculated by employing the computer program CompHEP, the phase space integrals by the Monte Carlo integrator and event generator BASES/SPRING. The dependence of the 4-fermion cross section on energy, Higgs boson mass and Higgs width is studied in detail. Interference contributions between the various diagrams are found not to alter significantly the production and decay distributions of the Higgs boson. It is shown that already the counting rate of the reaction $e^+e^- \longrightarrow \mu^+\mu^- b\bar{b}$ at LEP200 can provide evidence for the existence of the Higgs boson. The dependence of the $\mu^+\mu^- b\bar{b}$ cross section on the Higgs width will allow to extract information on this width in particular at LEP200 energies.

1 Introduction

It is well known that the Higgs boson is one of the most important but still not observed particles in the Standard Model (SM)[1]. Dominant properties of the SM like unitarity and renormaliziability are strongly connected with the existence of the Higgs boson, and fermions and gauge bosons become massive due to their interactions with the Higgs particle. Therefore, the search for the Higgs boson and the probing of its couplings with other fields is one of the major reasons for a future linear collider to be constructed.

However, the mass of the Higgs is not predicted by the SM, and the strategy of the Higgs search depends crucialy on the mass region where the search is performed. The present limit of the Higgs mass based on LEP100 data is $M_H >$ 60 GeV [2]. The mass interval 65 GeV $\leq M_H \leq$ 100 GeV including the region $M_H \simeq M_Z$ will hopefully be covered by the LEP200 collider [3].

A Higgs with a mass $M_H \geq 2M_Z$ may be easily discovered at the future hadron colliders SSC and LHC, either in the *golden* decay mode $H^0 \longrightarrow 2Z \longrightarrow \mu^+\mu^-\mu^+\mu^-$ or in the *silver* decay mode [4] $H^0 \longrightarrow 2Z \longrightarrow \mu^+\mu^-$2-jets. Searches for an intermediate mass Higgs boson with $M_Z \leq M_H \leq 2M_Z$ are rather difficult at such machines because of the large background expected. Detailed studies showed that the only hope is in looking for a signal in the rare decay [4] $H^0 \longrightarrow \gamma\gamma$. Unfortunately, the event numbers expected are small and, in addition, the detection requires a very precise measurement of the photon energies and directions.

Recently Higgs searches have been discussed in the mass region $M_Z \leq$ 100 - 110 GeV at the TEVATRON collider in the process [5] $p\bar{p} \longrightarrow Wb\bar{b} + X$. In this

case a signal can be expected if the luminosity of the $p\bar{p}$ collider is increased up to about 500 pb^{-1}, and a highly efficient b-jet tagging system is available.

The best prospects for the detection of a light or intermediate Higgs particle are offered by e^+e^- colliders like LEP200 or a possible Next Linear Collider (NLC)[1]. We would like to stress that as a consequence of the clean background conditions in particular the NLC will play a unique role for a detailed investigation of the Higgs sector, namely the couplings with other particles, the spin-parity and the Higgs self interaction. Probing of the couplings requires however a calculation of the Higgs production cross section with the best accuracy possible.

It is well known that the bremsstrahlung process [6]

$$e^+e^- \longrightarrow H^0Z \tag{1}$$

is dominant at cms energies less than ~500 GeV; in particular for LEP200 it is the only feasible reaction for discovery of the Higgs. The WW-fusion mechanism of the Higgs production

$$e^+e^- \longrightarrow \nu\bar{\nu}H \tag{2}$$

will be most important above ~0.5 TeV (see [7] and ref.'s therein).

One promising possibility in searching for the light or intermediate Higgs boson is the study of the reaction

$$e^+e^- \longrightarrow \mu^+\mu^- b\bar{b}. \tag{3}$$

Experimentally the H^0Z final state, with $H^0 \to b\bar{b}$ as the dominant decay mode, leads to $e^+e^-\, b\bar{b}$, $\mu^+\mu^-\, b\bar{b}$, $\tau^+\tau^- b\bar{b}$, $\nu\bar{\nu}b\bar{b}$ and 2-jet $b\bar{b}$ 4-body final states. The cleanest event signature coupled with very small background is expected for the $\mu^+\mu^-\, b\bar{b}$ final state.

Reaction (1) for the Higgs production has been calculated taking into account the 1-loop electroweak corrections [8]. Monte Carlo simulations of the process (1) including the main background sources, with different decay modes of H^0 and Z, have been reported in [9] using the program PYTHIA 5.6 and JETSET 7.3 [10]. These simulations took the effects of initial state radiation and the important gluon corrections to the partial width of the decay $H^0 \to b\bar{b}$ [7] into account.

However, all simulations have been carried out in the approximation of $2 \to 2$ processes for the Higgs signal and the background reactions, incoherently added:

$$e^+e^- \longrightarrow ZH^0,\ e^+e^- \longrightarrow ZZ,\ e^+e^- \longrightarrow \gamma^*\gamma^*,\ e^+e^- \longrightarrow Z\gamma^* \tag{4}$$

[1]Next Linear Collider is used as generic name for all linear e^+e^- collider designs presently under study.

with off-shell Z, γ^* and H^0 decays in the final state.

Actually a complete description of reaction (3) requires the consideration of all possible diagrams and interferences which contribute to the 4-fermion final state $\mu^+\mu^- b\bar{b}$. These contributions may significantly influence the H^0 detection probability and the determination of its properties.

In this paper we present the calculation of the complete set of relevant diagrams in the Born approximation. In particular, in sect. 2 we study the behaviour of the cross section of reaction (3) as a function of the cms energy and the Higgs mass. Invariant $b\bar{b}$ mass distributions are also shown in order to indicate the H^0 detection potential of future e^+e^- colliders. Emphasis has been directed towards obtaining information on the total width of the H^0 from $\mu^+\mu^- b\bar{b}$ cross section measurements, especially at LEP200 energies. Sect. 3 presents the study of the interference terms and their possible influence on the Higgs production and decay properties. The final chapter is devoted to a summary of this paper.

2 Properties of the reaction $e^+e^- \longrightarrow \mu^+\mu^- b\bar{b}$ and its behaviour near H^0Z and ZZ thresholds

The precise knowledge of the $\mu^+\mu^- b\bar{b}$ cross section for the process (3) which involves the bremsstrahlung reaction (1) as a subchannel, is important because of the rather low statistics expected especially at LEP200 and, if the Higgs particle has been discovered, for probing the couplings H^0ZZ and $H^0b\bar{b}$. Therefore it is necessary to consider, in addition to the electroweak corrections to the signal reaction $e^+e^- \to H^0Z$, the complete set of diagrams leading to the 4-body final state $\mu^+\mu^- b\bar{b}$.

A part of this task has been considered in ref. [11] for the process

$$e^+e^- \longrightarrow b\bar{b}Z, \tag{5}$$

which involves a subset of the diagrams necessary to describe process (3) completely. In particular, the rather important background contributions $e^+e^- \to \gamma^*\gamma^*$ ($\gamma^* \to \mu^+\mu^-$, $\gamma^* \to b\bar{b}$) were not taken into account.

The calculation of the process (3), $e^+e^- \longrightarrow \mu^+\mu^- b\bar{b}$, has been performed using the computer program CompHEP [12] and the Monte Carlo integrator and event generator BASES/SPRING [13]. The generation of the Feynman diagrams, the analytical calculations of the matrix element squared and their optimised Fortran code is done with the package CompHEP, while the Monte Carlo integration over phase space and the corresponding generation of the event flow are done with the package BASES/SPRING. The event flow obtained has

been incorporated into the program package PYTHIA as a *new* process, so that we could use all advantages of that program in the following.

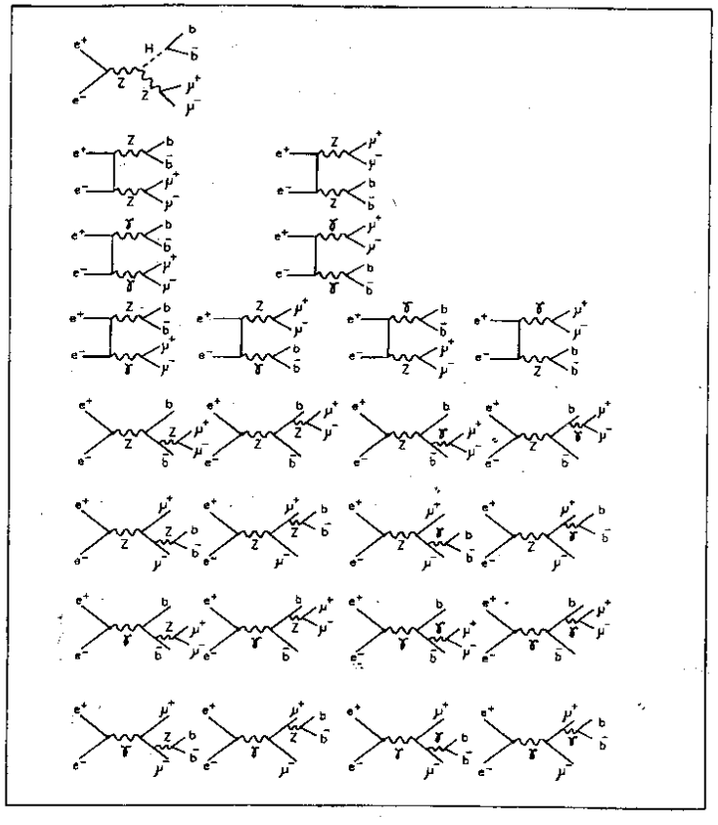

Figure 1: Diagrams contributing to the reaction $e^+e^- \longrightarrow \mu^+\mu^- b\bar{b}$.

The diagrams contributing to the process (3) are presented in Fig. 1. The first diagram corresponds to the Higgs signal reaction (1), with the decays $H^0 \rightarrow b\bar{b}$ and $Z \rightarrow \mu^+\mu^-$. The two diagrams of the second row correspond to the main background contribution:

$$e^+e^- \longrightarrow ZZ\,(Z \rightarrow \mu^+\mu^-,\ Z \rightarrow b\bar{b}). \qquad (6)$$

The diagrams in the third and fourth row correspond to background connected with the virtual Z, γ^* or γ^*-pair production with the subsequent decays to $\mu^+\mu^-$ and $b\bar{b}$:

$$e^+e^- \longrightarrow Z\gamma^*\,(Z \rightarrow \mu^+\mu^-,\ \gamma^* \rightarrow b\bar{b}\ or\ Z \rightarrow b\bar{b},\ \gamma^* \rightarrow \mu^+\mu^-) \qquad (7)$$

$$e^+e^- \longrightarrow \gamma^*\gamma^*\,(\gamma^* \rightarrow \mu^+\mu^-\,, \gamma^* \rightarrow b\bar{b}). \qquad (8)$$

The remaining 16 diagrams involve Z or γ^* radiation from a muon or $b(\bar{b})$-quark line with decays to $b\bar{b}$ or $\mu^+\mu^-$. These diagrams are s-channel type diagrams whereas the diagrams in rows 2-4 are of t-channel type. Diagrams with H^0 radiation from a muon line or with $H^0 \rightarrow \mu^+\mu^-$ decay are omitted in Fig. 1. Their contributions have been calculated and found to be negligible ($<.01\%$). This can be understood since the Yukawa couplings of the Higgs boson are proportional to the fermion masses.

The calculation of the diagrams in Fig. 1 has been made taking into account the non zero-masses of all fermions in the final state. Breit-Wigner denominators have been used for the Higgs and Z bosons in the intermediate states. The results presented for the cross sections have been obtained with restrictions in the $\mu^+\mu^-$ and $b\bar{b}$ invariant masses. A cut on $M_{\mu^+\mu^-}$ is used in order to reduce a large background contribution. We have choosen $M_{\mu^+\mu^-} > 12$ GeV and $M_{b\bar{b}} > 12$ GeV.

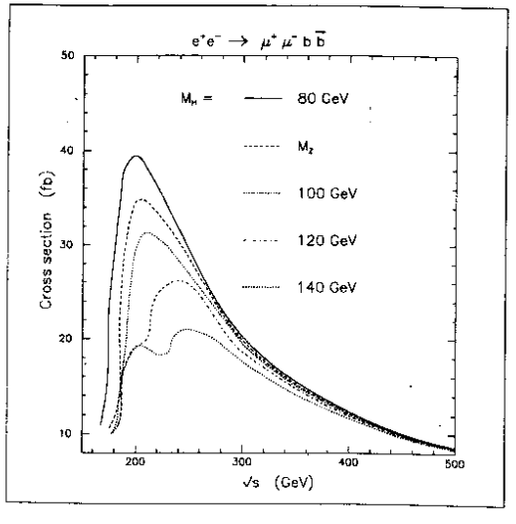

Figure 2: Cross section of the reaction $e^+e^- \longrightarrow \mu^+\mu^- b\bar{b}$ versus cms energy for different values of the Higgs mass M_H, with $M_{\mu^+\mu^-} > 12$ GeV and $M_{b\bar{b}} > 12$ GeV.

The cross sections for reaction (3) calculated with the SM parameters and the tree-level Higgs width are presented in Fig. 2 as a function of the cms energy

$\sqrt{s}$ for different values of the Higgs mass. One notices the typical threshold behaviour: a fast rise and a 1/s fall-off at large energies. In addition, a two-peak structure appears if the Higgs mass is ~120 GeV or larger which is due to the onset of the dominant 2-to-2 body reactions $e^+e^- \to ZZ$ and $e^+e^- \to H^0Z$ at different thresholds. For $M_H < 120$ GeV, both reaction thresholds are close to each other and no distinct two-bump structure appears. It is interesting to note the size of the $\mu^+\mu^- b\bar{b}$ cross section itself near threshold for H^0 masses ≤ 100 GeV. E.g. at $\sqrt{s}$= 200 GeV, i.e. at LEP200, the 4-body final state cross section is about 50% larger if an H^0 with $M_H = 100$ GeV exists than without a Higgs, and twice as large for $M_H = 80$ GeV. Hence, just counting the events of the reaction $e^+e^- \longrightarrow \mu^+\mu^- b\bar{b}$ can provide a first hint for the existence of the Higgs boson.

$\sqrt{s}(GeV)$	M_H (GeV)				
	80	M_Z	100	120	140
160	10.5	10.1	10.0	10.0	10.0
170	12.6	9.8	9.6	9.6	9.6
180	29.5	11.7	10.5	10.3	10.3
190	38.4	30.1	18.7	17.1	17.0
200	39.6	34.5	29.7	19.2	19.1
300	20.2	19.9	19.5	18.6	17.6
500	8.65	8.62	8.59	8.47	8.38

Table 1: Cross sections (in fb) for the process $e^+e^- \longrightarrow \mu^+\mu^- b\bar{b}$ for different Higgs masses and cms energy values, with $M_{\mu^+\mu^-} > 12$ GeV and $M_{b\bar{b}} > 12$ GeV.

Some $\mu^+\mu^- b\bar{b}$ cross section values for different energies and Higgs masses are collected in Table 1. The influence of the cut in $M_{\mu^+\mu^-}$ has been investigated by recalculating the cross sections with $M_{\mu^+\mu^-} > 1$ GeV instead of 12 GeV and without a cut in the $\mu^+\mu^-$ invariant mass. For $M_H = 80$ GeV and $\sqrt{s}$= 200 GeV, the cross sections increases to 58.2 fb and 68.0 fb, respectively. At $\sqrt{s}$= 160 GeV, where H^0 production is strongly suppressed, σ increases to 41.4 fb and 66.4 fb, respectively. Comparison with Table 1 shows that a large part of the γ^* background contribution is rejected by requiring $M_{\mu^+\mu^-} > 12$ GeV. Removing the cut $M_{b\bar{b}} > 12$ GeV does however not change the cross sections by more than 0.7%.

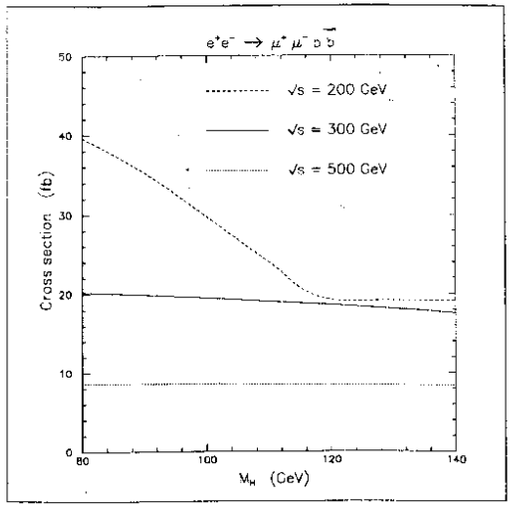

Figure 3: Cross section of the reaction $e^+e^- \longrightarrow \mu^+\mu^- b\bar{b}$ as a function of the Higgs mass M_H for different cms energies, with $M_{\mu^+\mu^-} > 12$ GeV and $M_{b\bar{b}} > 12$ GeV.

Fig. 3 shows the variation of the cross section $\sigma(e^+e^- \longrightarrow \mu^+\mu^- b\bar{b})$ with respect to the Higgs mass. As can be seen, for $\sqrt{s}$= 200 GeV the cross section lowers by a factor of ~2 from $M_H = 80$ GeV to $M_H = 140$ GeV, whereas above LEP200 energies σ does not depend strongly on the Higgs mass. At $\sqrt{s}$= 500 GeV, the cross section is practically not affected by Higgs mass variation up to 140 GeV.

In Fig. 4 the $b\bar{b}$effective mass distributions are presented for cms energy values of $\sqrt{s}$= 200, 300 and 500 GeV. Higgs masses were assumed to be at 80, 110 and 140 GeV. In these distributions the $\mu^+\mu^- b\bar{b}$ event numbers, with $M_{\mu^+\mu^-} > 12$ GeV and $M_{b\bar{b}} > 12$ GeV, have been normalized to the integrated luminosity

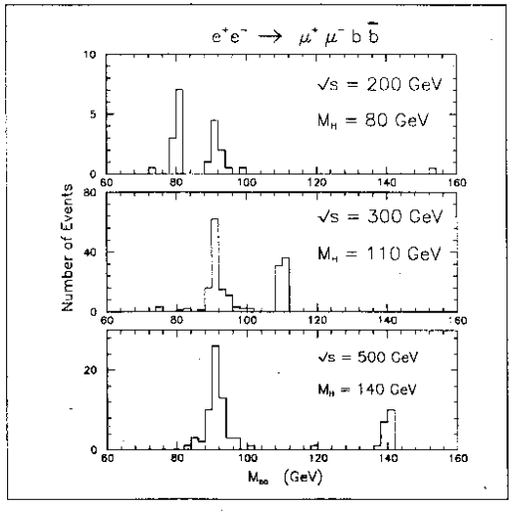

Figure 4: Invariant $b\bar{b}$ mass distributions at cms energies of 200, 300 and 500 GeV. The number of events are normalized to the expected luminosities for LEP200 and NCL, respectively, with $M_{\mu^+\mu^-} > 12$ GeV and $M_{b\bar{b}} > 12$ GeV.

of 500 fb^{-1} for LEP200 and 10 fb^{-1} for the NLC. Clear peaks are visible for the Higgs and Z bosons despite the rather small number of events expected. Background contributions are very small.

It is well known that the total width Γ_H of the H^0 is below 10 MeV for $M_Z \leq$ 140 GeV. Therefore, a direct measurement of Γ_H from the $b\bar{b}$ invariant mass distribution is not possible. However, it is an interesting challenge whether the variation of the $\mu^+\mu^- b\bar{b}$ cross section can give information on Γ_H.

In the package CompHEP the Fortran code for the matrix elements squared is obtained with the mass and width of the Higgs particle as independent parameters. The user has then the choice to fix the width Γ_H either to the value predicted in the minimal Standard Model, or to introduce some other value. In all calculations presented so far the tree-level value of Γ_H has been used. In the following we investigate how the cross section $\sigma(e^+e^- \longrightarrow \mu^+\mu^- b\bar{b})$ changes when the Higgs width Γ_H is modified in some way.

Fig. 5 shows, for three Higgs mass values, the $\mu^+\mu^- b\bar{b}$ cross section at $\sqrt{s}$= 200 GeV as a function of the Higgs width. The variation with Γ_H is significant: the cross section falls rapidly when the width is growing by only a few MeV. The effect is more pronounced at lower Higgs masses.

In Fig. 6 the cross section for production of the $\mu^+\mu^- b\bar{b}$ final state is shown

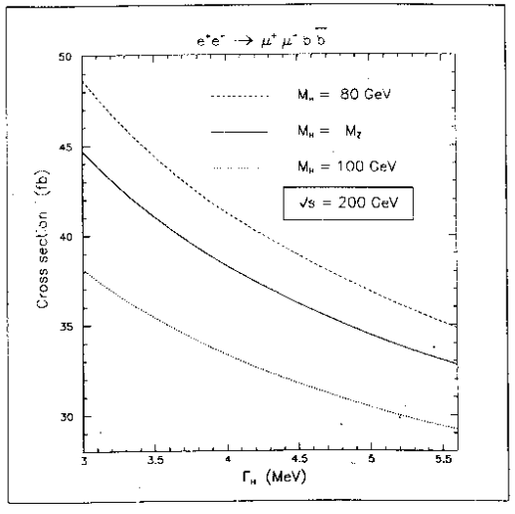

Figure 5: Cross section of the reaction $e^+e^- \longrightarrow \mu^+\mu^- b\bar{b}$ versus the Higgs width Γ_H for different Higgs masses at cms energy of 200 GeV, with $M_{\mu^+\mu^-} > 12$ GeV and $M_{b\bar{b}} >$ 12 GeV.

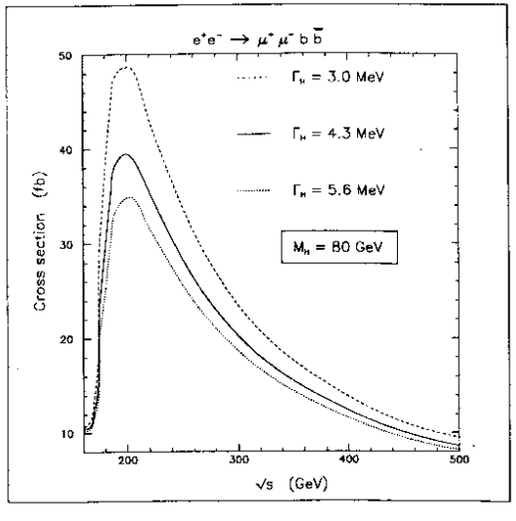

Figure 6: Cross section of the reaction $e^+e^- \longrightarrow \mu^+\mu^- b\bar{b}$ versus cms energy for different Higgs widths, with $M_{\mu^+\mu^-} > 12$ GeV and $M_{b\bar{b}} > 12$ GeV.

as a function of $\sqrt{s}$ for $M_H = 80$ GeV and three Γ_H values. A change by $\pm$ 30% from the tree level value of $\Gamma_H = 4.3$ MeV modifies the cross section quite drastically, especially in the $\sqrt{s}$ range from 175 to ~240 GeV. As an example, at $\sqrt{s}$= 200 GeV and $M_H = 80$ GeV, the cross section decreases from 49 fb to 40 fb if Γ_H grows from 3.0 to 4.3 MeV. Hence, a cross section measurement with an accuracy of about 20% for reaction (3) at LEP200 would yield the possibility to determine the H^0 width with ~30% uncertainty. Of course, one can try to measure Γ_H only if the Higgs has been found and its mass is determined rather well.

3 Interference terms and s-channel Z/γ^* radiation diagrams

In the previously published studies and simulations of the Higgs signal and background processes, $e^+e^- \to H^0Z$ and $e^+e^- \to Z(\gamma^*)Z(\gamma^*)$, the calculations were carried out by

- adding the corresponding diagrams incoherently and
- omitting the diagrams with Z/γ^* radiation from a muon or $b(\bar{b})$ quark leg (the diagrams of rows 5-8 in Fig. 1).

The off-shell Z, γ^* and H^0 particles were then allowed to decay to $Z(\gamma^*) \to \mu^+\mu^-$ or $b\bar{b}$ and $H^0 \to b\bar{b}$. To understand whether these approximations are sufficient, especially with regard to the investigation of Higgs production and decay properties, we compare the results of the complete set of diagrams in Fig. 1 with those of the following approximation: only the diagrams from the first 4 rows in Fig. 1 are considered, and the diagrams of each row are added coherently. In this way we involve only interference terms which lead to the same intermediate 2-body final state. This approximation is very close to previous simulation procedures for searches and studies of the Higgs boson. The main difference which remains is that instead of subsequent 2 to 2- and 1 to 2-body phase space integrations we integrate a priori over the whole 4-body phase space.

A detailed comparison of the calculation of the two sets of diagrams is presented for three examples:

- $\sqrt{s} = 200$ GeV, $M_H = 80$ GeV
- $\sqrt{s} = 200$ GeV, $M_H = M_Z$
- $\sqrt{s} = 500$ GeV, $M_H = 140$ GeV

with $M_{\mu^+\mu^-} > 12$ GeV and $M_{b\bar{b}} > 12$ GeV.

The first two cases are relevant for LEP200 energies, while the last example may be of interest for NLC studies. The energy chosen is in any case larger than the H^0Z and ZZ thresholds so that their production is not restricted by phase space boundaries.

Let us denote the cross section of the complete set of diagrams as σ_{compl}, and the cross section in the approximation as described above as σ_{appr}. In order to reduce the statistical error of the comparison to a very small or negligible amount, large number of event samples of the 4-fermion final state $\mu^+\mu^- b\bar{b}$ were generated.

Concerning the total $\mu^+\mu^- b\bar{b}$ cross section, σ_{compl} and σ_{appr} turn out to be very similar. The largest cross section difference of 0.2% is found in the case of $\sqrt{s}$= 200 GeV and $M_H = M_Z$, whereas at 500 GeV no difference is seen at all. Hence, interference terms and all s-channel Z/γ^* radiation diagrams can be neglected in overall cross section estimations for cms energies above the ZZ/H^0Z thresholds. At lower $\sqrt{s}$ the difference between σ_{compl} and σ_{appr} is in the order of a few percent. For example, at $\sqrt{s}$= 170 GeV and $M_H = 140$ GeV, $\sigma_{compl} = (9.56 \pm 0.07)$ fb and $\sigma_{appr} = (9.25 \pm 0.03)$ fb.

However, interference patterns may occur in differential distributions such that after integration over phase space the effects are cancelled.

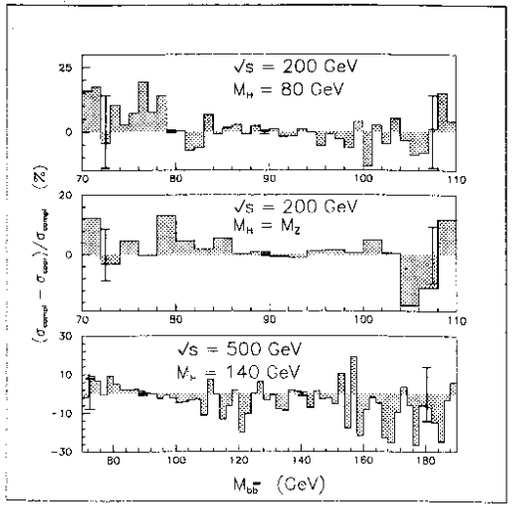

Figure 7: $b\bar{b}$ invariant mass distribution for the difference of the cross sections σ_{compl} and σ_{appr}, normalized to σ_{compl}.

Fig. 7 shows the difference of the cross sections σ_{compl} and σ_{appr} , normalized to σ_{compl},

$$\Delta\sigma = \frac{\sigma^i_{compl} - \sigma^i_{appr}}{\sigma^i_{compl}} * 100\%, \qquad (9)$$

where i denotes the i-th bin, as a function of the $b\bar{b}$ invariant mass. Also indicated are some one-standard deviation errors. In general, significant deviations from zero cannot be observed. Non-zero values may occur under the Z peak at $\sqrt{s}$= 200 GeV (for M_H = 80 GeV, $\Delta\sigma$ = (2 ± 0.8)% and for $M_H = M_Z$, $\Delta\sigma$ = (0.5 ± 0.1)%). Such effects come from the diagrams with Z boson radiation from a muon (see Fig. 1). These diagrams contribute less with increasing energy so that they are negligible at 500 GeV, in agreement with our calculations.

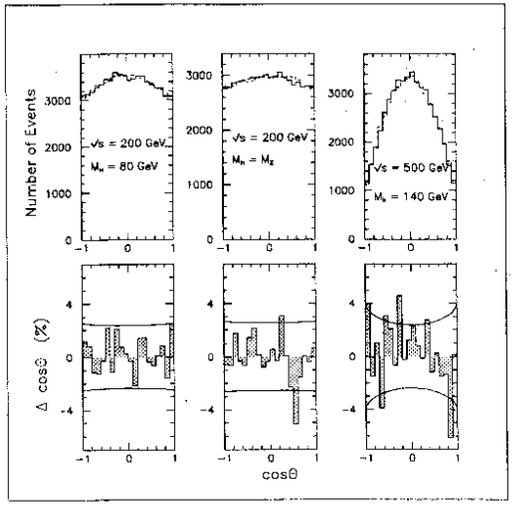

Figure 8: H^0 production angular distributions, cosΘ(Z,beam), of the reaction $e^+e^- \rightarrow H^0Z$ and the difference of the cross sections σ_{compl} and σ_{appr}, normalized to σ_{compl}.

Information of the spin-parity of the Higgs boson can be extracted from its production and decay angular distributions. By selecting only events with $M_{b\bar{b}}$ around the nominal H^0 mass, $M_{H^0} - 3\Gamma_{H^0} < M_{b\bar{b}} < M_{H^0} + 3\Gamma_{H^0}$, a very clean sample of $e^+e^- \rightarrow H^0Z$ events can be obtained. The exception is case 2 where this simple mass cut leads to a mixture of H^0Z and ZZ events. We present in Fig. 8 the production angular distributions, cosΘ(Z,beam), for the complete (full histogram) and approximated (dotted histogram) calculations and in Fig. 9 the b-quark polar angle distributions in the rest frame of the Higgs boson, cosΘ(b-quark,H^0) as well as the normalized differences of the two calculations. The curves represent the one-standard deviation error margins.

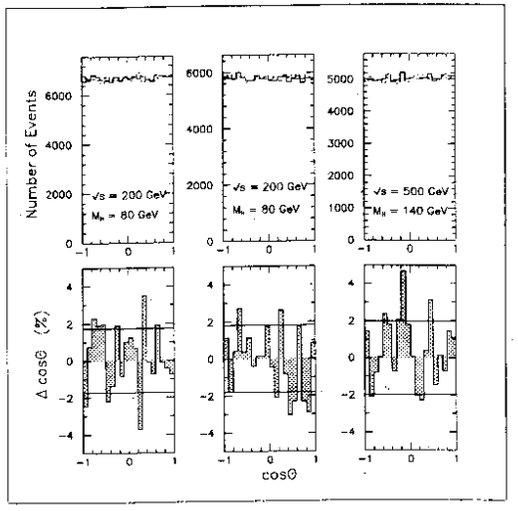

Figure 9: b-quark decay angular distributions, cosΘ(b-quark,H^0), of the reaction $e^+e^- \rightarrow H^0Z \rightarrow b\bar{b}Z$ and the difference of the cross sections σ_{compl} and σ_{appr}, normalized to σ_{compl}.

As can be seen, the production angular distributions reveal a $\cos^2\Theta$ component, which is more pronounced at higher energies, and an isotropic behaviour for the b-quark as seen in the H^0 rest frame. This is in accord with the expectations for a spin-zero Higgs boson. The difference distributions are in all cases consistent with zero over the whole range. Thus, interference terms as well as the s-channel Z/γ^* radiation diagrams do not influence the Higgs boson production and decay characteristics significantly. Their omission in previous studies of Higgs production has therefore not led to serious errors, as shown by our calculations.

4 Conclusions

In this paper we present the calculations of the complete set of Born-type diagrams in the minimal Standard Model contributing to the process $e^+e^- \longrightarrow \mu^+\mu^- b\bar{b}$. This 4-fermion final state is one of the most promising event signatures for the search of a Higgs boson with mass below ~140 GeV at LEP200 and NLC energies.

It has been shown that the dominant contributions to the $\mu^+\mu^- b\bar{b}$ final state come from the Higgs signal bremsstrahlung diagram and the t-channel background diagrams with $ZZ, Z\gamma^*$ and $\gamma^*\gamma^*$ production and subsequent decay to $\mu^+\mu^-$ and $b\bar{b}$. The remaining diagrams of Fig. 1 as well as the interference terms give only small contributions; in particular above the ZZ and H^0Z thresholds and with the cuts $M_{\mu^+\mu^-} > 12$ GeV, $M_{b\bar{b}} > 12$ GeV they are less than ~0.2% and hence negligible. In energy regions below these thresholds they contribute with a few percent.

The behaviour of the cross section $\sigma(e^+e^- \longrightarrow \mu^+\mu^- b\bar{b}\,)$ at LEP200 energies shows that the number of events expected will be twice as large if a Higgs boson with a mass of 80 GeV exists, compared with the case of no Higgs, or ~50% larger if M_H is close to 100 GeV. Therefore, just counting the $\mu^+\mu^- b\bar{b}$ events will provide indirect evidence on the existence of the Higgs boson. For energies above ~200 GeV the effect of the Higgs on the cross section will become smaller, decreasing to about 20% at 500 GeV.

The $b\bar{b}$ invariant mass distributions of the 4-fermion final state has been presented for $\sqrt{s}$= 200, 300 and 500 GeV, assuming a Higgs boson with masses of 80, 110 and 140 GeV, respectively. Normalizing to the number of events expected according to the design luminosities of the colliders, clear peaks from the H^0 are visible. This observation confirms conclusions of previous studies.

Attention has been given to the question whether the diagrams neglected in previous studies, as well as possible interference terms, will affect the production and decay angular distributions to be studied in connection with the Higgs boson. It has been demonstrated that these terms do not significantly alter the corresponding angular distributions expected for a spin-zero particle, and that therefore their contributions can be fully neglected in studies of the Higgs signal.

An interesting feature of the reaction $e^+e^- \longrightarrow \mu^+\mu^- b\bar{b}$ is the rather strong dependence of the cross section on the total Higgs width Γ_H, especially in the LEP200 energy region. The standard procedure to measure the width of a short-lived particle from the invariant mass distribution of its decay products seems to be excluded for the Higgs boson, since Γ_H is less than 10 MeV for $M_H \leq 140$ GeV and the measurement therefore is completely determined by the detector resolution. Information on Γ_H may however extracted to an accuracy of ~30% if the cross section of reaction (3) is measured with a 20% error.

We end by emphasizing that all our considerations are based on tree-level calculations. We are aware that a thorough study should include electroweak and QCD corrections as well as a realistic detector simulation. The aim of this paper was to study the contributions of diagrams omitted so far, the interference pattern between all of them, and their impact on the appearence of the Higgs signal. We conclude that the complete set of all possible tree diagrams and their interferences for the reaction $e^+e^- \longrightarrow \mu^+\mu^- b\bar{b}$ is very well approximated at LEP200 and NLC energies by the incoherent sum of the bremsstrahlung Higgs production diagram and the $Z(\gamma^*)Z(\gamma^*)$ background contributions with subsequent $H^0 \rightarrow b\bar{b}$, $Z/\gamma^* \rightarrow b\bar{b}\,/\mu^+\mu^-$ decays.

5 Acknowledgements

We are grateful to M. Dubinin for useful discussions and V. Ilyin and A. Pukhov for the help with CompHEP calculations. Two of us (E.B. and S. Sh.) would like to thank P. Soeding for his interest and support, DESY-IfH Zeuthen and the Zeuthen L3 group for the kind hospitality.

References

[1] S.L. Glashow, Nucl. Phys. **22** (1961) 579;
S. Weinberg, Phys. Rev. Lett. **19** (1967) 1264;
A. Salam, Elementary Particle Theory, ed. N. Svartholm, Stockholm (1968), 367.

[2] The L3 collaboration, O. Adriani et al., preprint CERN-PPE/93-31, 1993, to be submitted to Phys. Lett. **B**;
S.C.C. Ting, preprint CERN-PPE/93-34, 1993.

[3] S. L. Wu et al., Proc. of the ECFA workshop, Aachen 1988, CERN Report 87-08;
R. Kleiss, Z. Kunszt and W. J. Stirling, Phys. Lett. **242B** (1990) 507;
N. Brown, Z. Phys. **C49** (1991) 657.

[4] J. F. Gunion and G. L. Kane, Proc. of the 1990 summer Study on High Energy Physics, 1990, Snowmass, Colorado, p. 59.

[5] E. Boos et al., D0 note 1719/93, FNAL, 1993.

[6] J. D. Bjorken, Proc. of the 1976 SLAC Summer Inst. on Particle Physics, SLAC Report, B106(1976) 292;
J. Ellis et al., Nucl. Phys. **B106** (1976) 292;
B. L. Joffe and V. A. Khoze, Phys. of Elem. Part. and At. Nucl. (USSR)9 (1978) 118.

[7] A. Djouadi et al., Proc. of the Workshop - Munich, Annecy, Hamburg, 1991, DESY Report 92-123A, p. 11.

[8] J. Fleischer and F. Jegerlehner, Nucl. Phys. **B216** (1983) 469;
A. Denner, B. A. Kniehl and J. Kúblbeck, Proc. of the Workshop - Munich, Annecy, Hamburg, 1991, DESY Report 92-123A, p. 31.

[9] P. Grosse-Wiesmann, D. Haidt and H. J. Schreiber, Proc. of the Workshop Munich, Annecy, Hamburg, 1991, DESY Report 92-123A, p. 37.

[10] T. Sjöstrand, PYTHIA 5.6 and JETSET7.3, Preprint CERN-TH. 6488/92.

[11] E. E. Boos and M. N. Dubinin, Preprint NPI MSU 92-41/290, to be submitted to Phys. Lett. **B**.

[12] E. E. Boos et al. Proc. of the XXVIth Recontre de Moriond, ed. by J. Tran Than Van, Edition Frontiers, 1991, p. 501;
E. E. Boos et al., Proc. of the Second Int. Workshop on Software Engineering, ed. by D. Perred-Gallix, World Scientific, 1992, p. 665;
E. E. Boos et al., KEK Preprint 92-47, 1992.

[13] S. Kawabata, Comp. Phys. Commun. **41** (1986) 127.